Articles

The Structure of the Monomeric Porcine Odorant Binding Protein Sheds Light on the Domain Swapping Mechanism‡

Silvia Spinelli,§ Roberto Ramoni,|| Stefano Grolli,|| Jacques Bonicel,⊥ Christian Cambillau,§ and Mariella Tegoni*,§

Architecture et Fonction des Macromolécules Biologiques, UPR 9039, CNRS, IFR1, 31 Chemin Joseph Aiguier, 13402 Marseille Cedex 20, France, Istituto di Biochimica Veterinaria, Facoltà di Medicina Veterinaria, Università di Parma, Via del Taglio 8, 43100 Parma, Italy, and Bioénergétique et Ingénierie des Protéines, UPR 9036, CNRS, IFR1, 31 Chemin Joseph Aiguier, 13402 Marseille Cedex 20, France

Received January 23, 1998; Revised Manuscript Received April 1, 1998

ABSTRACT: The X-ray structure of the porcine odorant binding protein (OBPp) was determined at 2.25 Å resolution. This lipocalin is a monomer and is devoid of naturally occurring bound ligand, contrary to what was observed in the case of bovine OBP [Tegoni, M., et al. (1996) *Nat. Struct. Biol. 3*, 863−867; Bianchet, M. A., et al. (1996) *Nat. Struct. Biol. 3*, 934−939]. In this latter protein, a dimer without any disulfide bridges, domain swapping was found to occur between the β- and α-domains. A single Gly (121) insertion was found in OBPp when it was compared to OBPb, which may prevent domain swapping from taking place. The presence of a disulfide bridge between the OBPp β- and α-domains (cysteines 63 and 155) may lock the resulting fold in a nonswapped monomeric conformation. Comparisons with other OBPs indicate that the two cysteines involved in the OBPp disulfide bridge are conserved in the sequence, suggesting that OBPp may be considered a prototypic OBP fold, and not OBPb.

Many of the events associated with olfaction are still poorly understood at a molecular level (*1*). It is known however that odorants are in general small hydrophobic molecules and have to travel from air to olfactory receptors in neurones (*2*) through the aqueous compartment of nasal mucus (*3*). Several components of the nasal mucus of vertebrates have been isolated, which are presumably involved in interactions with odorant molecules and olfactory receptors. These components include a highly abundant class of proteins, the odorant binding proteins (OBPs), with a binding affinity for some odorant molecules, which has been identified and characterized. The bovine odorant binding protein (OBPb) was the first member of this family to be described (*4*−*6*). On the basis of amino acid sequence comparisons, OBPb was classified as belonging to the lipocalin family (*7*, *8*). The intriguing structure of OBPb, which has been solved by X-ray crystallography (*9*, *10*), revealed an unsuspected feature, since the fold typical of lipocalins is complicated in this case by the swapping (*11*) of the α-helical domain of the one monomer over the β-barrel of the second monomer. The absence of any disulfide bridges and the presence of a salt bridge at the hinge region (Glu125−Arg96) have been thought to provide a reasonable explanation for the extension of the α-helix arm (*9*) as well as for the monomerization reported to occur at acidic pH (*12*). Other OBPs were later detected in the nasal mucosa of frog (*13*), rat (*14*), rabbit and pig (*15*), mouse (*16*), and porcupine (*17*). We have decided to investigate the OBP from pig nasal mucosa (OBPp), taken as an example of a functional monomer (*18*). OBPp is also a lipocalin, and it has been reported to have a pattern of affinity for various odors similar to that of OBPb. Its affinity was found in the classical pyrazine binding assay to be higher than that of OBPb under comparable experimental conditions [0.5 and 3.0 μM (*18*)], and its affinity for a wide range of nutty and green-smelling odorants has been amply documented (*18*, *19*). Here we report on the structure of porcine OBP at 2.25 Å resolution. The presence of a single glycine insertion (Gly121) at the interdomain hinge and that of a disulfide bridge locking the molecule may explain why domain swapping is not observed in OBPp. These structural features and the sequence similarity with OBPb make OBPp a good candidate for designing point mutations at amino acids likely to be involved in the domain swapping mechanism observed in OBPb (*11*, *20*).

MATERIALS AND METHODS

Protein Purification and Amino Acid Sequence Determination. Pig OBP was purified from fresh pig nasal mucosa by combining two procedures previously used on the porcine (*15*) and bovine (*5*) proteins with modifications. Nasal mucosa samples were taken from freshly slaughtered animals (typically 30 g/animal) and immediately homogenized (War-

‡ The coordinates have been deposited with the Brookhaven Protein Data Bank under code 1A3Y.

* Corresponding author. Phone: (33) 91 16 45 01. Fax: (33) 91 16 45 36. E-mail: tegoni@afmb.cnrs-mrs.fr.

§ UPR 9039, CNRS.

|| Università di Parma.

⊥ UPR 9036, CNRS.

S0006-2960(98)00179-2 CCC: $15.00
Published on Web 05/13/1998

ing blendor) in 2 volumes of 20 mM Tris-HCl at pH 7.8 (buffer A). The suspension, after centrifugation (40000*g*, 30 min), was subjected, in sequence, to the following steps: ammonium sulfate cut (pig OBP-containing fraction from 60 to 100% saturation), acidification (to pH 4.1 by addition of 1 M citric acid), neutralization (to pH 7.8 by addition of 1 M Tris base), and overnight dialysis (against buffer A). The extract was filtered (0.22 μm) and loaded onto a FPLC column filled with the anion-exchange resin Baker Bond Wide Pore PEI (NH) equilibrated in buffer A containing 0.3 M NaCl. The elution was performed with a 0.3 to 1 M NaCl gradient, and the pig OBP-containing fractions (0.90−1.0 M NaCl) were pooled and dialyzed overnight against buffer A. The solution was then loaded onto a Mono Q column (Pharmacia-FPLC) equilibrated in buffer A and eluted with a gradient of NaCl from 0 to 0.5 M. The peak eluted at 0.36 M salt exhibited in SDS−PAGE a single 28 kDa band corresponding to pure pig OBP (*15*). The protein was dialyzed again against buffer A, concentrated to 10 mg/mL (Centricon CF 25 concentrator, Amicon), and stored at −20 °C. The degree of purification was evaluated after each step by SDS−PAGE analysis under reducing conditions. The average purification yield was about 0.3 mg of pig OBP per gram of nasal mucosa.

The molecular mass of native pig OBP was determined by performing gel permeation on a Superdex 70 FPLC column. Pig OBP was eluted in a single peak at 25 kDa, in agreement with previously published data (*15*). Native pig OBP behaves like a monomer but showed a molecular mass higher than that predicted on the basis of the amino acid sequence (19 kDa). The molecular mass of the denatured protein was determined with two different PAGE protocols both under reducing conditions [2.5% (v/v) β-mercaptoethanol] and with different percentages of SDS (1.5 and 5.0%), and values of 28 and 18 kDa were obtained. No significant degree of glycosylation was detected with any of the methods used.

Part of the amino acid sequence determination was carried out on a purified OBP from pig after proteolytic (Arg-C and trypsin) and chemical (CNBr) treatment. The peptide fragments were separated by HPLC with a linear gradient of acetonitrile from 6 to 90%. Major peaks in a first run of chromatography frequently required a second separation. Amino acid analyses were carried out either with a Beckman model 6300 autoanalyzer or by high-pressure liquid chromatography using the Pico-Tag method. In both cases, samples were hydrolyzed at 116 °C over the course of 24 h under vacuum by vapor of 6 N HCl. Automated Edman degradation was performed on an Applied Biosystems model A470 gas-phase sequencer with on-line analysis of the phenylthiohydantoin derivatives. Approximately 300 pmol of protein and 20−1000 pmol of peptides were applied on Beckman protein and peptide supports, respectively. *N*-Methylpiperidine was used as the coupling base for Edman sequencing. The amino acid sequence kindly provided by P. Pelosi et al. (S. Paolini, A. Scaloni, Marchese, Napolitano, and P. Pelosi, submitted for publication, SwissProt number P81245) gave us the possibility to complete regions still lacking in our determination and to confirm those already in our hands.

Crystallization and Data Collection. Pig OBP was crystallized by vapor diffusion at 20 °C, at a protein concentration of 8 mg/mL in the presence of 2 M ammonium sulfate and 5% 2-propanol. The crystals belong to the orthorhombic space group $P2_12_12_1$ with the following cell dimensions: $a = 42.6$ Å, $b = 88.7$ Å, and $c = 93.2$ Å. With two molecules per asymmetric unit, the specific protein volume $V_m = 2.3$ Å^3 Da^{-1} (46% of the solvent) (*21*).

Table 1: Data Collection and Final Refinement Statistics

Data Collection	
resolution limit (Å)	30.0−2.15
data completion [$I/\sigma(I) > I$] (%)	99.4
% with $I > 3\sigma(I)$	83.8
redundancy	5
R_{sym} (all/last shell)[a] (%)	5.1/26.5
Refinement	
resolution limit (Å)	25.0−2.25
number of reflections	21750
number of protein atoms	2328
number of water molecules	197
final *R*-factor/*R*-free[b] (%)	18.1/24.7
B-factor (Å^2)	
main chains (molecules A/B)	39.2 (33.1/45.2)
side chains (molecules A/B)	39.6 (34.2/45.3)
solvent	40.1
rms deviation from ideal value	
bonds (Å)	0.008
angles (deg)	1.36
improper/dihedral angles (deg)	1.10/ 26.7

[a] $R_{sym} = \Sigma[\Sigma|I(h)_i - \langle I(h)\rangle|/\Sigma\langle I(h)\rangle]/n$, where $I(h)_i$ is the observed intensity of the *i*th measurement of reflection *h* and $\langle I(h)\rangle$ the mean intensity of reflection *h*. [b] $R = \Sigma|F_o - F_c|/\Sigma|F_o|$, where F_o and F_c are the observed and calculated structure factor amplitudes, respectively.

Before the data collection, the crystals were soaked for a few seconds in a reservoir solution containing 2 M ammonium sulfate and 27% (v/v) glycerol and were then rapidly frozen at 100 K. A set of 100° oscillation data was collected at 2.15 Å resolution and 100 K on a MAR-Research Imaging Plate (J. Hendricks and A. Lenfer, Hamburg, Germany) placed on a Rigaku RU200 rotating anode using a copper target. The data sets were integrated with the Denzo program and merged (*22*). The data collection and integration statistics are given in Table 1.

Structure Resolution and Refinement. The structure of pig OBP was determined by performing molecular replacement with AMoRe (*23*), using OBPb as the starting model. The solution of the molecular replacement procedure for the two molecules was the first of the list after the translation−fitting step of AMoRe, with a correlation coefficient of 30.4% and an *R*-factor of 48.9% (between 8.0 and 3.5 Å). The rotated models were fitted and adjusted into σ-weighted electron density maps (*24*). Refinement was performed using the XPLOR slow-cooling procedure (*25*), with data between 22.0 and 2.25 Å. Cycles of X-PLOR refinement were alternated with manual refitting into a σ-weighted electron density map with the graphic program Turbo-Frodo (Roussel & Cambillau, AFMB, Marseille, France). As the low-resolution data were employed in the refinement, a low-resolution bulk solvent correction was applied, as implemented in the XPLOR program version 3.843 (*26*). The final OBPp model has an *R*-factor of 18.1% and an *R*-free of 24.7%, in the 25.0−2.25 Å range (Table 1). The $(F_{obs} - F_{calc})\exp(i\alpha_{calc})$ maps (*24*) did not show any uninterpretable features. The final model consisted of 2328 non-hydrogen protein atoms and 197 water molecules. The final model has excellent geometry according to the PROCHECK criteria (*27*) with

```
          1         10        20        30        40
                              ß1 +              + + +   ß2
OBPP  ----EEPQPEQDP FELSGKWITS YIGSSDLEKI GENAPFQVFM RSIEFDDKES
OBPB  ---AQEEEAEQNL SELSGPWRTV YIGSTNPEKI QENGPFRTYF RELVFDDEKG
MUP   -EEASSTGRNFNV EKINGEWHTI ILASDKREKI EDNGNFR-LF LEQIHVLEN-
OBPR1 TDPAHHENLDISP SEVNGDWRTL YIVADNVEKV AEGGSLRAYF QHMECGDECQ

          50        60        70        80        90
          ß3 + +     ß4     + +     ß5 + +   + +   ß6    ß7
OBPP  KVYLNFFSKE NGICEEFSLI GTK-QEGNTYD VNYAGNNKFV VSYASE-TALI
OBPB  TVDFYFSVKR DGKWKNVHVK ATK-QDDGTYV ADYEGQNVFK IVSLSR-THLV
MUP   SLVLKFHTVR DEECSELSMV ADKTEKAGEYS VTYDGFNTFT IPKTDYDNFLM
OBPR1 ELKIIFNVKL DSECQTHTVV GQK-HEDGRYT TDYSGRNYFH VLKKTDD-IIF

          100       110       120       130       140       150   157
          + +       ß8 +++ +          α                ß9
OBPP  ISNINVDEEG DKTIMTGLLG KGTDIEDQDL EKFKEVTREN GIPEENIVNI IERDDCPA
OBPB  AHNINVDKHG QTTELTGLFV K-LNVEDEDL EKFWKLTEDK GIDKKNVVNF LENENHPHPE
MUP   IFLIN-EKDG ETFQLMGLYG REPDLSSDIK ERFAQLCEEH GILRENIIDL SNANRCLQARE
OBPR1 AHNVNVDESG RRQCDLVAGK RE-DLNKAQK QELRKLAEEY NIPNENTQHL VPTDTCNQ
```

FIGURE 1: Sequence alignment of porcine OBP (this study), bovine OBP, MUP, and rat OBP1. Residue types common to three proteins are in red, and those common to all four proteins are green. Those which are also common to OBPp and OBPb are light blue. The secondary structure elements are indicated by continuous lines, and the residues forming the internal cavity are identified with a +.

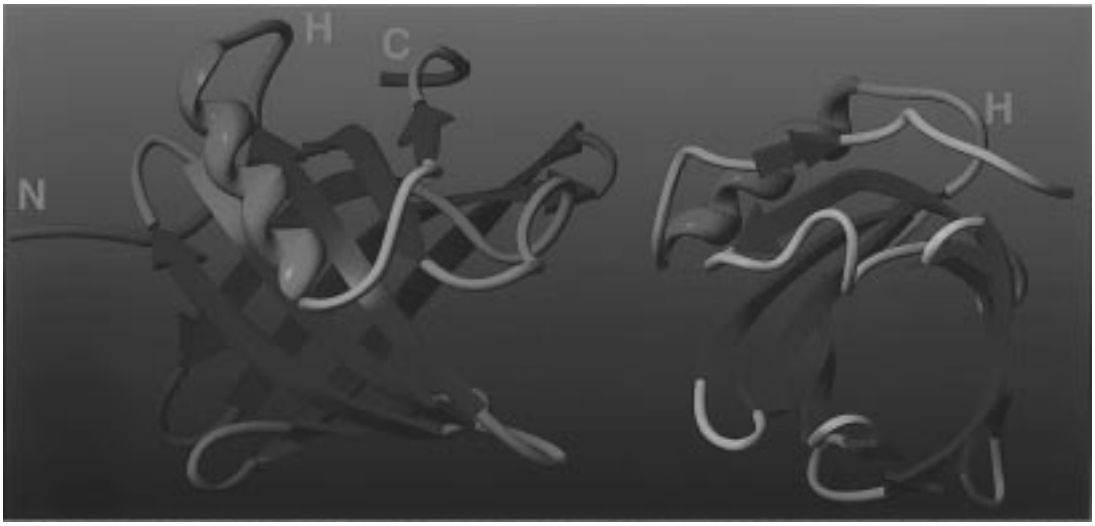

FIGURE 2: Three-dimensional structure of porcine OBP. (a, left) The β-barrel is indigo, and the helix is red; the letter H indicates the hinge segment. (b, right) Structure from part a turned at an angle of roughly 90°.

85% of the residues located in the most favorable area, 15% in additional allowed regions, and no residues in forbidden zones. The OBPp coordinates have been deposited with the Brookhaven Protein Data Bank (PDB entry 1A3Y).

RESULTS AND DISCUSSION

Overall Structure. In solution, the functional OBPp has been described as a monomer with an apparent molecular mass ranging from 18 to 28 kDa (ref *15* and this work) showing no sign of dimerization, contrary to what was observed with bovine OBP (*5*). On the basis of protein sequence data (P. Pelosi, personal communication), OBPp was found to contain 157 amino acids and its sequence identity with OBPb and rat major urinary protein (MUP) is 42.3 and 26.7%, respectively (Figure 1). Two cysteines forming a disulfide bridge were found to occur in the amino acid sequence at positions 63 and 155 (Figure 1). The three-dimensional structure of OBPp was determined, using as a starting model the structure of bovine OBP β-barrel A and α-domain B, to reconstitute the classical lipocalin-like fold (*9*, *10*). As in the classical lipocalin fold, each OBPp monomer is composed of a nine-stranded β-barrel comprising residues 9−120 (strands 1−8) linked by a turn (residues 121−123) to a short α-helical domain (residues 124−141) followed by the ninth β-strand (146−148) and the C-terminal tail (residues 149−157) (Figure 2). The N-terminal segment (residues 1−8) is not visible in the electron density map, probably because it is flexible. Although OBPp is monomeric in solution, two molecules are present in the crystal asymmetric unit, but no domain swapping has been found to occur in this lipocalin. Molecule A and molecule B consist of amino acids 9−157 and 12−157, respectively. The two monomers contact each other face to back and are tilted at an angle of roughly 90° along an axis which is perpen-

FIGURE 3: Comparison between porcine and bovine OBPs. (a, left) Porcine OBP (pink) superimposed on the bovine OBP dimer (green and yellow). (b, right) Comparison between the OBPb extended monomer (green) superimposed on that of OBPp (pink).

dicular to the axis of the β-barrel. The surface area of the dimer interface was found to account for only 2.6% of the total area of the dimer (400 Å^2 out of a total area of 14 500 Å^2), a value which is far below the limit generally thought to apply to dimers of biological significance (*28*). In OBPb, where domain swapping was observed (Figure 3), the dimer interface area was found to be 2500 Å^2 (out of a total area of 15 000 Å^2). When monomer A was superimposed on monomer B, an rms deviation of 0.47 Å was obtained with 145 Cα atoms. This value is quite low, considering the large number of Cα atoms taken into account in the comparison. The largest deviations were detected in the loop regions of residues 24−35 (0.6−1.5 Å), 59−62 (0.8−1.2 Å), 73−77 (0.6−0.8 Å), 93−97 (0.8 Å), 106−110 (0.6−0.7 Å), 122−125 (0.7−1.2 Å), and 138−145 (0.9−1.1 Å). The *B*-factor values were much higher (average value = 45.3 Å^2) in molecule B than in molecule A (average value = 33.6 Å^2). The cysteine residues (63 and 155) form a disulfide bridge between the C terminus and the loop joining strands 3 and 4 of the β-barrel, comparable to that observed in MUP (*29*) and S-RBP (*30*) (residues 68−161 in MUP and 70−174 in S-RBP). This disulfide bridge is conserved in all the lipocalin sequences identified so far, from bacteria to mammals (*31*), with one exception, that of bovine OBP. The rms deviation observed between OBPp and the other lipocalins after superimposition is also quite low: 0.60 Å with OBPb (with 90 Cα atoms included in the comparison) and 0.60 Å with MUP (84 Cα atoms).

Why Does Domain Swapping Not Occur in Porcine OBP? An explanation for the absence of domain swapping in OBPp can be found upon examining the stretch of residues which separates its two domains (residues 117−126); in OBPp, the separating turn is located within the sequence L^{117}LGK**G**^{121}-TDIED^{126}, where Gly121 is a major component of the turn (Figure 1). The corresponding sequence in OBPb is L^{118}-FVK-LNVED^{126}, in which the residues at the extremities have high sequence identities, but where the essential glycine is absent (Figure 1). It has been previously reported that domain swapping may occur or be induced when the length of the segment joining the swappable domains is reduced (*11*). Upon examination of the superimposed linkers in the three-dimensional structures of OBPb-A, OBPb-B, and OBPp (Figure 4), it can be seen that the structural data are in full agreement with what was suggested by the sequence alignment. Glycine 121 is located exactly at a position where domain swapping occurs in OBPb, and in addition, it induces a shift in the alignment of the structural elements of the three protein chains included in the comparison (Figure 4). OBPb domain swapping might therefore occur because the linker segment is shorter and less flexible than in OBPp. In other OBPs, the lack of strong sequence homologies in this segment prevents any conclusions from being drawn. Furthermore, the absence of cysteines in OBPb may prevent any nonswapped forms from stabilizing, which is not the case for other OBPs, which all have cysteines in a good position for forming a disulfide bridge.

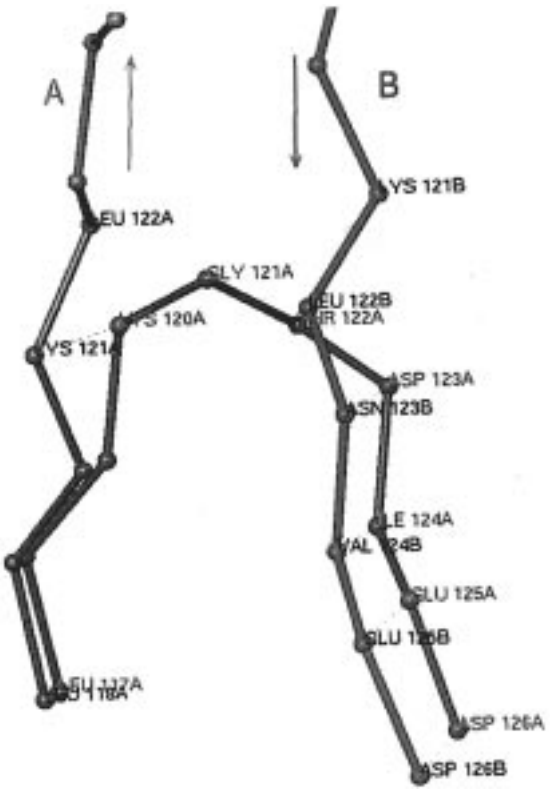

FIGURE 4: Closeup of the hinge region of OBPb (yellow, A; green, B) superimposed on that of OBPp (red), showing the insertion of Gly121 into OBPp as compared with OBPb.

In MUP, the linker segment has the same length as that present in OBPp and contains a proline at a residue position following that of Gly121 in OBPp. In rat OBPs, the situation

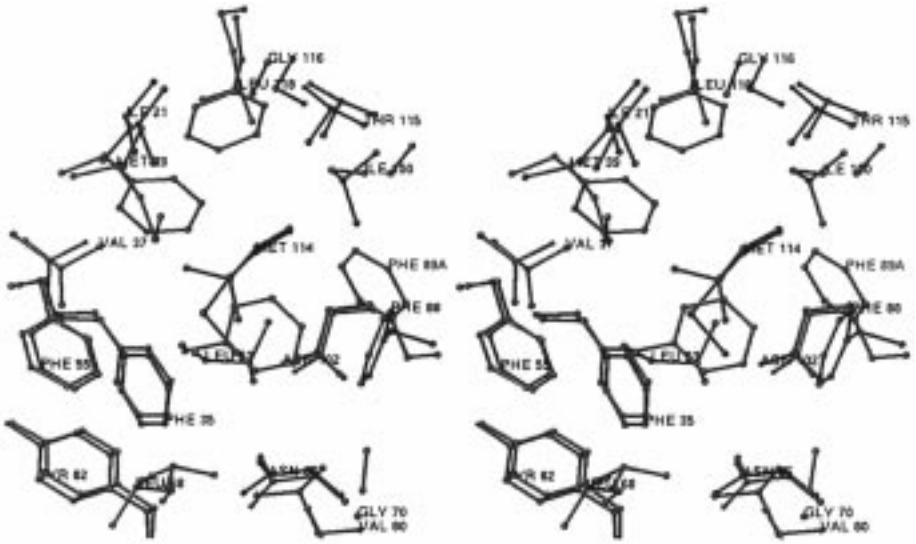

FIGURE 5: Stereoview of the residues forming the hydrophobic cavity in the β-barrel (bovine OBP is green, porcine OBP is pink; numbering corresponds to that of porcine OBP, except for bovine OBP Phe89).

is very different. Rat OBP1 has a linker length identical to that of OBPb, but since the degree of sequence identity is very remote, valid comparisons cannot be made in this case. A similar situation was found to occur in rat OBP2, where the sequence identity was even lower and where a large deletion occurs after this segment. The presence of the conserved disulfide bridge in both rat OBPs might however favor the structure being the nonswapped kind.

The β-Barrel Internal Cavity. Upon calculation of the water accessible surface of OBPp, a single cavity was observed inside the β-barrel, as previously described in OBPb (*9*, *10*) and MUP (*29*). Contrary to what occurs in these two lipocalins, where naturally occurring ligands were detected in the cavity, no significant electron density was observed in the OBPp internal cavity, indicative of the absence of bound ligand. A faint density patch was observed at the center of the cavity, far from its walls, which was modeled by a water molecule. Alternatively, this patch of density may have resulted from the central parts of ligands being bound in a disordered way and giving rise to partial occupancy. The dimensions of the cavity are equivalent to those of OBPb; its surface area is 510 Å^2, compared with 520 Å^2 in the case of OBPb. As previously noted with MUP (*29*) and OBPb (*9*, *10*), the cavity does not communicate directly with the external solvent, since a few amino acid side chains block the channel leading to the outside, and will no doubt be required to move for the binding between the protein and odors to be possible. As was to be expected, the residues forming the cavity of the β-barrel (Figure 5) are mainly hydrophobic (Ile21, Val37, Met39, Leu53, Leu68, Gly70, Val80, Ile100, Met114, Gly116, and Leu118) and aromatic (Phe35, Phe55, Tyr82, and Phe88), while only a few of them are polar-uncharged (Thr37, Asn86, Asn102, and Thr115). These residues are mostly located within the β-strands of the barrel or adjacent to them (Figure 1). Some side chain substitutions have occurred as can be seen when this sequence is compared with the OBPb cavity. Thr37 has been replaced by Val, Phe39 by Met, Phe53 by Leu, Val68 by Leu, Ala70 by Gly, Ala80 by Val, Ala100 by Ile, Leu114 by Met, and Phe118 by Leu (Figures 1 and 5). These substitutions do not however significantly affect the hydrophobic and aromatic character of the cavity compared with that of OBPb, as was to be expected from the binding data in solution (*18*, *19*). Only four of the 18 residues forming the cavity are conserved in the four OBP and MUP sequences (Figure 1); five are found in three sequences, and the remaining nine occur only once or twice. Side chain polarity inversion was detected in only four places. The naturally occurring ligand modeled in OBPb would be able to fit into the OBPp cavity without any major constraints, except in two places; it would clash with residues Val80 (Ala in OBPb) and Phe88 (conserved, Phe89 in OBPb). Phenylalanine 89 has been found to have a flexible side chain (ref *10* and unpublished work of M. Tegoni et al.) in OBPb. When bound to 2-amino-4-butyl-5-propylselenazole, carvone, or pyrazine (M. Tegoni et al., unpublished), the Phe89 side chain undergoes a 120° rotation around its χ_1 angle to prevent a clash from occurring with these cyclic compounds, despite the fact that they do not occupy the whole cavity. The naturally occurring ligand in OBPb has been thought on the contrary to be a noncyclic molecule, which is compatible with Phe88 being in another position. In OBPp, where the cavity was found to be empty, the position of Phe88 side chain corresponds to that observed in OBPb complexes with the cyclic compound, resulting from a side chain rotation from the position observed in the naturally occurring complex.

Significance of the Structure. Bovine OBP was for a long time viewed as the prototypic OBP and was extensively studied by performing binding assays. The occurrence of domain swapping and the fact that OBPb is functional only as a dimer seem to make this unusual protein rather difficult to understand, however. Contradictory results and interpretations have been published due to the fact that one ligand odor was apparently bound per OBP dimer in solution (*5*, *12*). It was suggested that binding might occur inside the lipocalin barrel as well as in a pocket formed at the dimer interface by the swapped domain structure (*9*), the existence of which may explain the stoichiometry of one odor per dimer observed in solution (*5*, *12*). Alternatively, it was hypothesized that binding might occur at both of the lipocalin sites in solution, but with very different affinities (*32*). The

high-affinity ligand would be almost impossible to remove; therefore, only the low-affinity site would be accessible for ligand substitution in a micromolar concentration range. When the structure of OBPb was solved, the question was partly answered. Bianchet et al. (*10*) established that, in the crystal, two odor molecules (one per monomer) could replace the naturally occurring ligand found in the β-barrel cavity. We identified an open cavity however between the swapped domains of the OBPb dimer and proposed that this cavity might be used for odor transport, or alternatively, to house another ligand (*9*). Our data on OBPp suggest that the most plausible OBP odor binding site is located inside the β-barrel, since this may generally be the only possibility in OBPs, with the exception of OBPb. The intriguing fact that OBPb exhibits domain swapping and possesses a third interdimer open cavity suggests that this protein may have some other function. OBPs have been found so far to possess the cysteine residues which form the disulfide bridge in OBPp. All the members of the OBP family probably exhibit a classical lipocalin fold and an odor binding site located in the closed β-barrel cavity. Protein engineering experiments on the two closely related bovine and porcine OBPs would make it possible to explain the role of the shorter linker and the absence of a disulfide bridge in the OBPb domain swapping mechanism.

ACKNOWLEDGMENT

We thank Paolo Pelosi, Sara Paolini, and Andrea Scaloni for provinding us with the OBPp sequence prior to publication and Paolo Pelosi and Enrico Bignetti for helpful discussions. We thank Sabine Diotallevi, Philippe Cantau, and Carlos Carranza for their technical assistance, and we are grateful to Gino Tegoni for kindly providing us with pig nasal mucosa.

REFERENCES

1. Pelosi, P. (1994) Odorant-Binding Proteins, *Crit. Rev. Biochem. Mol. Biol. 29*, 199−228.
2. Buck, L., and Axel, R. (1991) *Cell 65*, 175−187.
3. Pevsner, J., Sklar, P. B., Hwang, P. M., and Snyder, S. H. (1989) *Chem. Senses 1*, 227−242.
4. Pelosi, P., Baldaccini, N. E., and Pisanelli, A. M. (1982) *Biochem. J. 201*, 245−248.
5. Bignetti, E., Cavaggioni, A., Pelosi, P., Persaud, K. C., Sorbi, R. T., and Tirindelli, R. (1985) *Eur. J. Biochem. 149*, 227−231.
6. Pevsner, J., Trifiletti, R. R., Strittmatter, S. M., and Snyder, S. H. (1985) *Proc. Natl. Acad. Sci. U.S.A. 82*, 3050−3054.
7. Cavaggioni, A., Sorbi, R. T., Keen, J. N., Pappin, D. J. C., and Findlay, J. B. C. (1987) *FEBS Lett. 212*, 225−228.
8. Tirindelli, R., Keen, J. N., Cavaggioni, A., Eliopoulos, E. E., and Findlay, J. B. C. (1989) *Eur. J. Biochem. 185*, 572−589.
9. Tegoni, M., Ramoni, R., Bignetti, E., Spinelli, S., and Cambillau, C. (1996) *Nat. Struct. Biol. 3*, 863−867.
10. Bianchet, M. A., Bains, G., Pelosi, P., Pevsner, J., Snyder, S. H., Monaco, H. L., and Amzel, L. M. (1996) *Nat. Struct. Biol. 3*, 934−939.
11. Bennet, J. M., Schlunegger, M. P., and Eisenberg, D. (1995) *Protein Sci. 4*, 2455−2468.
12. Bussolati, L., Ramoni, R., Grolli, S., Donofrio, G., and Bignetti, E. (1993) *J. Biotechnol. 30*, 225−230.
13. Lee, K. H., Wells, R. G., and Reed, R. R. (1987) *Science 253*, 1053−1056.
14. Dear, T. N., Campbell, K., and Rabbitts, T. H. (1991) *Biochemistry 30*, 10376−10382.
15. Dal Monte, M., Andreini, I., Revoltella, R., and Pelosi, P. (1991) *Comp. Biochem. Physiol. 99B*, 445−451.
16. Pes, D., Dal Monte, M., Ganni, M., and Pelosi, P. (1992) *Comp. Biochem. Physiol. 103B*, 1011−1017.
17. Felicioli, A., Ganni, M., Garibotti, M., and Pelosi, P. (1993) *Comp. Biochem. Physiol. 105B*, 775−784.
18. Dal Monte, M., Centini, M., Anselmi, C., and Pelosi, P. (1991) *Chem. Senses 18*, 713−721.
19. Hérent, M.-F., Collin, S., and Pelosi, P. (1995) *Chem. Senses 20*, 601−608.
20. Bergdoll, M., Remy, M.-H., Cagnon, C., Masson, J.-M., and Dumas, P. (1997) *Structure 5*, 391−400.
21. Matthews, B. W. (1968) *J. Mol. Biol. 33*, 491−497.
22. Otwinovski, Z. (1993) *DENZO: an oscillation data processing program for macromolecular crystallography*, Yale University Press, New Haven, CT.
23. Navaza, J. (1994) *Acta Crystallogr. A50*, 157−163.
24. Read, R. J. (1986) *Acta Crystallogr. A42*, 140−149.
25. Brunger, A. T., Kuriyan, J., and Karplus, M. (1987) *Science 35*, 458−460.
26. Brunger, A. T. (1996) *Xplor version 3.843 manual*, Yale University Press, New Haven, CT.
27. Laskowski, R., MacArthur, M., Moss, D., and Thornton, J. (1993) *J. Appl. Crystallogr. 26*, 91−97.
28. Jones, S., and Thornton, J. M. (1995) *Prog. Biophys. Mol. Biol. 63*, 31−65.
29. Böcskei, Z., Groom, C. R., Flower, D. R., Wright, C. E., Phillips, S. E. V., Cavaggioni, A., Findlay, J. B. C., and North, A. C. T. (1992) *Nature 360*, 186−188.
30. Cowan, S. W., Newcomer, M. E., and Jones, T. A. (1990) *Proteins 8*, 44−61.
31. Flower, D. R., Sansom C. E., Beck, M. E., and Attwood T. K. (1995) *Trends Biochem. Sci. 20*, 498−499.
32. Pevsner, J., Hou, V., Snowman, A. M., and Snyder, S. H. (1990) *J. Biol. Chem. 265*, 6118−6125.

BI980179E